Dual-contrast computed tomography enables detection of equine posttraumatic osteoarthritis in vitro

Saukko, Annina E.A.; Nykänen, Olli; Sarin, Jaakko K.; Nissi, Mikko J.; te Moller, Nikae C.R.; Weinans, Harrie; Mancini, Irina A.D.; Visser, Jetze; Brommer, Harold; More Authors

DOI
10.1002/jor.25066

Publication date
2021

Document Version
Final published version

Published in
Journal of Orthopaedic Research

Citation (APA)
Saukko, A. E. A., Nykänen, O., Sarin, J. K., Nissi, M. J., te Moller, N. C. R., Weinans, H., Mancini, I. A. D., Visser, J., Brommer, H., & More Authors (2021). Dual-contrast computed tomography enables detection of equine posttraumatic osteoarthritis in vitro. *Journal of Orthopaedic Research*, *40*(3), 703-711. https://doi.org/10.1002/jor.25066

Received: 18 March 2021 | Accepted: 26 April 2021

DOI: 10.1002/jor.25066

RESEARCH ARTICLE

Journal of Orthopaedic Research®

Dual-contrast computed tomography enables detection of equine posttraumatic osteoarthritis in vitro

Annina E. A. Saukko[1,2] | Olli Nykänen[1,3] | Jaakko K. Sarin[1,4] | Mikko J. Nissi[1,3] | Nikae C. R. te Moller[5] | Harrie Weinans[6,7] | Irina A. D. Mancini[5] | Jetze Visser[7] | Harold Brommer[5] | P. Réné van Weeren[5] | Jos Malda[5,7] | Mark W. Grinstaff[8] | Juha Töyräs[1,4,9,10]

[1]Department of Applied Physics, University of Eastern Finland, Kuopio, Finland

[2]Department of Medical Physics, Turku University Hospital, Turku, Finland

[3]Research Unit of Medical Imaging Physics and Technology, University of Oulu, Oulu, Finland

[4]Diagnostic Imaging Center, Kuopio University Hospital, Kuopio, Finland

[5]Department of Clinical Sciences, Faculty of Veterinary Medicine, Utrecht University, Utrecht, The Netherlands

[6]Department of Biomechanical Engineering, Delft University of Technology (TU Delft), Delft, The Netherlands

[7]Department of Orthopedics, University Medical Center Utrecht, Utrecht, The Netherlands

[8]Departments of Biomedical Engineering, Chemistry, and Medicine, Boston University, Boston, Massachusetts, USA

[9]School of Information Technology and Electrical Engineering, The University of Queensland, Brisbane, Australia

[10]Science Service Center, Kuopio University Hospital, Kuopio, Finland

Correspondence
Annina E. A. Saukko, MSc (Tech.), Department of Applied Physics, University of Eastern Finland, Kuopio 70210, Finland.
Email: annina.saukko@uef.fi

Funding information

Jenny and Antti Wihuri Foundation; Dutch Arthritis Association, Grant/Award Numbers: LLP-12, LLP-22; Jorma ja Märtha Sihvola Foundation; Academy of Finland, Grant/Award Numbers: 285909, 293970, 307932; Doctoral Program in Science, Technology and Computing (SCITECO, University of Eastern Finland)

Abstract

To prevent the progression of posttraumatic osteoarthritis, assessment of cartilage composition is critical for effective treatment planning. Posttraumatic changes include proteoglycan (PG) loss and elevated water content. Quantitative dual-energy computed tomography (QDECT) provides a means to diagnose these changes. Here, we determine the potential of QDECT to evaluate tissue quality surrounding cartilage lesions in an equine model, hypothesizing that QDECT allows detection of posttraumatic degeneration by providing quantitative information on PG and water contents based on the partitions of cationic and nonionic agents in a contrast mixture. Posttraumatic osteoarthritic samples were obtained from a cartilage repair study in which full-thickness chondral defects were created surgically in both stifles of seven Shetland ponies. Control samples were collected from three nonoperated ponies. The experimental (n = 14) and control samples (n = 6) were immersed in the contrast agent mixture and the distributions of the agents were determined at various diffusion time points. As a reference, equilibrium moduli, dynamic moduli,

[Correction added on 24 May 2021, after first online publication: the second and third author names were swapped.]

and PG content were measured. Significant differences ($p < 0.05$) in partitions between the experimental and control samples were demonstrated with cationic contrast agent at 30 min, 60 min, and 20 h, and with non-ionic agent at 60 and 120 min. Significant Spearman's rank correlations were obtained at 20 and 24 h ($\rho = 0.482–0.693$) between the partition of cationic contrast agent, cartilage biomechanical properties, and PG content. QDECT enables evaluation of posttraumatic changes surrounding a lesion and quantification of PG content, thus advancing the diagnostics of the extent and severity of cartilage injuries.

KEYWORDS

articular cartilage, cationic contrast agent, contrast-enhanced computed tomography, dual-contrast agent, dual-energy computed tomography, posttraumatic osteoarthritis

1 | INTRODUCTION

Osteoarthritis (OA) is a progressive joint disease characterized by a breakdown of articular cartilage and underlying bone, pain, stiffness, and impairment of joint function. Single and multiple traumas to the joint cause focal damage, and more specifically lead to abnormal mechanical function and biochemical alterations of cartilage. Trauma may not only lead to a local chondral defect but can also trigger changes in the surrounding cartilage, predisposing patients to developing posttraumatic OA (PTOA). To prevent or delay the progression of an acute injury into PTOA, surgical and pharmaceutical interventions are needed.[1,2] However, injuries must be first detected and assessed. After the injury, the time to develop clinical PTOA varies highly from as short as 2–5 years but for some injuries, the timeframe can be even longer.[1] The earlier the cartilage degeneration can be detected in the preclinical phase, the better are chances for effective treatment. The focus of this study is to evaluate a new contrast-enhanced computed tomography (CECT) technique for the detection of the initial changes in cartilage adjacent to chondral defects.

Magnetic resonance imaging (MRI) is an important imaging tool in cartilage damage diagnostics as it features excellent soft-tissue contrast and can assess proteoglycan (PG) content, collagen orientation, and water content.[3,4] Unfortunately, MRI has a relatively low spatial resolution in vivo (1–2 mm) and long image acquisition times with the length of a typical knee MRI protocol varying from 20 to 30 min.[4,5] As an alternative to MRI, CECT enables the detection of cartilage degeneration in acute injuries[6–10] and has recently been introduced in the clinic. The advantages of CECT over MRI include better spatial resolution (0.5–0.625 mm), shorter acquisition time (<1 min), lower costs, and better availability. Furthermore, changes in the bony structures are better visualized in computed tomographic (CT) images.

The CECT of the knee typically involves two subsequent CT scans acquired immediately (arthrography) and 45 min (delayed arthrography) after the intra-articular injection of a contrast agent.[6,7,10] The first scan allows segmentation of the articulating surface and lesions, while the second scan reveals internal cartilage changes related to the initiation of PTOA (e.g., increased water content and decreased PG content). In CECT, contrast agents enhance the contrast at the synovial fluid-cartilage interface since the natural contrast at this interface is almost nonexistent in CT. Contrast agents also enable the detection of degenerative changes by examining their uptake and partitioning in the cartilage.[11–16] The early degenerative changes of cartilage include PG loss, disruption of the superficial collagen network, and increased water content.[17,18] These changes increase the uptake of anionic contrast agent (most commonly ioxaglate), enabling the evaluation of the internal cartilage changes and degeneration.[19]

A recently introduced cationic contrast agent (CA4+) has a superior sensitivity for revealing tissue PG content at diffusion equilibrium compared with the currently used anionic contrast agents.[13,20–22] Cationic contrast agents distribute in cartilage proportionally to the PG content due to the electrostatic attraction caused by the negative fixed charge density of the PG molecules. At the onset of diffusion, cationic contrast agent diffusion is also controlled by two other degeneration-related factors: increased water content and decreased steric hindrance (i.e., the physical diffusion barrier formed by the dense collagen network and the interspersed PGs in the matrix). Degeneration of the extracellular matrix has opposite effects on the diffusion of cationic agents: the loss of PGs decreases the diffusion while the increased water content and decreased steric hindrance increase the diffusion. This phenomenon diminishes the sensitivity of detecting cartilage injuries and osteoarthritic degeneration at clinically feasible imaging time points (30 min up to 2 h after the administration of the contrast agent[6]).

We previously reported that this weakness in clinically feasible time points is minimized by employing a quantitative dual-energy CT (QDECT) technique, together with a contrast agent mixture consisting of cationic, iodinated contrast agent (CA4+) and nonionic, gadolinium-based contrast agent (gadoteridol).[23,24] In the mixture, the cationic contrast agent is sensitive to the changes in PG content and the non-ionic contrast agent is sensitive to the tissue water content and altered steric hindrance. Thus, with non-ionic agent, the effect of water content and altered steric hindrance into CA4+ diffusion can be assessed.

QDECT is based on dual-energy CT that exploits the "absorption k-edges," that is, sharp element-specific changes in the photoelectric X-ray absorption spectrum. In this method, the energies and filtration of the X-ray beam are selected so that the resulting X-ray energy spectra fall on both sides of either gadolinium (50.2 keV) or iodine (33.2 keV) k-edge. The technique enables simultaneous quantification of the uptake of cationic and non-ionic contrast agents in cartilage and, thus, improved diagnosis of cartilage degeneration and injuries.[23,24]

Previous research on QDECT has focused on studying cartilage injuries in lesion sites of osteoarthritic human cartilage and bovine cartilage with artificial injuries and degeneration ex vivo.[23–27] In this study, we extend our examinations from the lesion site to the surrounding tissue to evaluate the capability of the technique to reveal changes related to PTOA. This is of interest because the changes in the adjacent tissue are usually not as prominent as in the lesion site and, thus, the sensitivity of the QDECT method needs to be validated in this setting. Additionally, this is the first time the QDECT technique is being evaluated in an equine model. Specifically, we investigate the potential of the QDECT technique for monitoring posttraumatic degeneration in the cartilage surrounding surgically repaired lesions in the equine stifle joint. We hypothesize that simultaneous quantification of the cationic and non-ionic contrast agent partitions using the QDECT technique enables the detection of posttraumatic, degeneration-related changes in the tissue surrounding the lesions at clinically relevant diffusion time points and, hence, QDECT improves the quantitative diagnosis of posttraumatic degeneration.

2 | METHODS

2.1 | Sample extraction

In both femoropatellar joints of Shetland ponies ($N = 7$, age = 8.8 ± 3.5 years, 6 females and 1 male) two full-thickness cylindrical chondral lesions ($d = 9$ mm) were surgically created on the medial femoral ridges. The experiments were carried out in a surgical theater at the Equine Division of the Department of Clinical Sciences, Utrecht University, The Netherlands. The lesions were treated with different combinations of chondrons and mesenchymal stem cells in different carrier hydrogels. After a 12-month treatment period, the ponies were euthanized. Osteochondral samples, including the lesions and surrounding tissue, were extracted postmortem from the medial femoral ridge (Figure 1). In addition, to obtain a representative sample population, equivalent osteochondral samples were extracted from femoropatellar joints of healthy ponies ($N_{control} = 3$, age = 10.3 ± 4.7 years) obtained from a local abattoir (Van de Veen, Nijkerk, The Netherlands), resulting in a total of 20 samples (14 experimental and 6 control). Extracted samples were frozen at −20°C until biomechanical testing. We expect that, based on literature, this freeze-thaw cycle did not induce substantial changes in the structure, composition, or biomechanical properties of cartilage.[28] The number of samples was based on power calculations of the original cartilage repair study.[29] The measurement protocol was evaluated and approved by the Ethics Committee of Utrecht University for Animal Experiments in compliance with the Institutional Guidelines on the Use of Laboratory Animals (Permission DEC 2014. III.11.098).

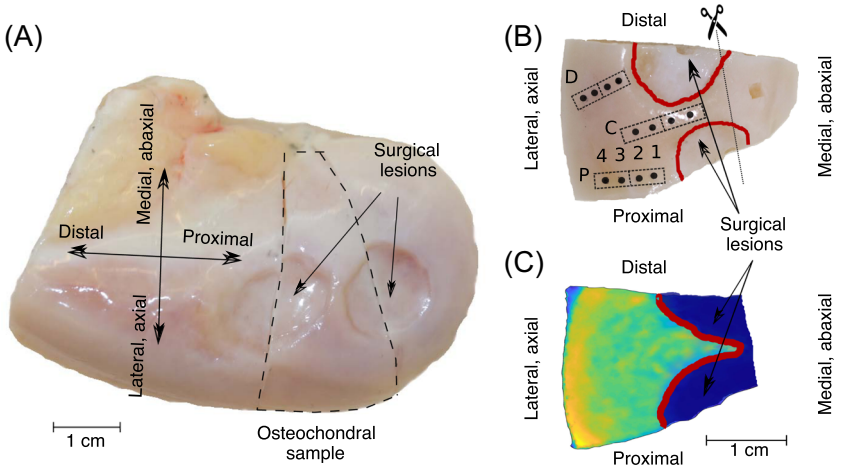

FIGURE 1 Sample extraction and anatomical locations. (A) Medial view of a left trochlea showing the locations of the surgically repaired lesions and the extraction site of an experimental sample. (B) Photograph of an experimental sample. Red lines indicate the locations of the surgically induced and repaired lesions. The boxes illustrate the locations where the histological samples were extracted, and the black dots illustrate the anatomical locations of the biomechanical measurement points. Letters P, C, and D (proximal, central, and distal) and numbers 1–4 denote the naming of the anatomical locations, for example, P1 is the proximal and closest location from the surgically repaired lesion. The line with scissors shows where the samples were trimmed before the microCT measurements. (C) Corresponding view of the CA4+ partition map [Color figure can be viewed at wileyonlinelibrary.com]

2.2 | Biomechanical testing

Biomechanical properties of cartilage were examined using indentation testing. Twelve biomechanical testing locations were examined from proximal (P), central (C), and distal (D) anatomical locations (Figure 1). Each anatomical location included four testing locations with the closest to a lesion denoted as location 1 and the farthest as location 4. A total of 235 locations were tested biomechanically (two samples had less than 12 locations due to the shape of the sample).[30] The indentation system utilized a 250 g load cell (accuracy ± 0.25%, Model 31; Honeywell Sensotec Sensors) and an actuator (displacement resolution 0.1 μm, PM500-1 A; Newport). During the measurements, the samples were glued to a custom-made sample holder and a perpendicular alignment with the face of a plane-ended nonporous cylindrical indenter (d = 0.53 mm) was ensured using a goniometer (Model #55-841; Edmund Optics Inc.). To begin with, the indenter was brought into contact with the sample. The contact was confirmed by indenting the sample five times using 2% strain. First, four stress-relaxation steps with 5% strain and a ramp velocity of 100%/s were performed using a relaxation time of 600 s in between the steps. Thereafter, dynamic sinusoidal loading (f = 1.0 Hz) with a strain amplitude of 1% was applied. The linear region of the stress-relaxation curve was used to determine the equilibrium modulus using Poisson's ratio of ν = 0.1. The dynamic modulus was calculated as a ratio of the stress and strain amplitudes obtained from the sinusoidal loading using a Poisson's ratio of ν = 0.5.[31,32] Measuring adjacent points with distances varying between 3 and 4 mm was feasible, as the diameter of the employed indenter was sufficiently small (~0.5 mm).

2.3 | MicroCT imaging

The QDECT measurements were conducted using a microCT scanner (Quantum FX; Perkin Elmer). The samples were scanned at room temperature using two X-ray tube voltages (90 and 50 kV) with a tube current of 200 μA and isotropic voxel size of 59 × 59 × 59 μm^3. Custom-made 2 mm and 0.588 mm copper filters were used in 90 and 50 kV scans, respectively. Each scan included seven calibration phantoms. These phantoms comprised of one distilled water phantom, three CA4 + (q = +4, M = 1499.17 g/mol) phantoms with iodine concentrations of 8, 16, and 32 mg I/ml, and three gadoteridol (q = 0, M = 558.69 g/mol, ProHance, Bracco Diagnostic Inc.) phantoms with gadolinium concentrations of 8, 16, and 32 mg Gd/ml. CA4+ was synthesized as reported previously.[14]

Before imaging, the sides and bottom of the osteochondral samples were sealed carefully using cyanoacrylate (Loctite, Henkel Norden AB), which served as a barrier and allowed the contrast agent diffusion only through the articulating surface. The X-ray attenuation within the cartilage was determined by imaging the osteochondral sample in air with both tube voltages. After baseline data acquisition, the samples were immersed in an isotonic (~308 mOsm/kg) mixture of CA4+ and gadoteridol diluted in phosphate-buffered saline (PBS). The iodine concentration in the solution was 10 mg I/ml, and the gadolinium concentration was 20 mg Gd/ml. The solution was supplemented with proteolytic inhibitors (5 mM ethylenediaminetetraacetic acid [EDTA; VWR International] and 5 mM benzamidine hydrochloride hydrate Sigma-Aldrich Inc.]) and penicillin–streptomycin (100 units/ml penicillin, 100 μg/ml streptomycin; Life Technologies) to prevent general protein degradation in the tissue. The samples were kept immersed in a contrast agent for 24 h in a bath volume of 20 ml at 7°C while the bath was stirred gently. The uptake of the dual-contrast agent in articular cartilage was imaged at five time points following an immersion period of 30 min, 1 h, 2 h, 20 h, and 24 h. The samples were imaged in air and the atmosphere in the imaging tube was kept moist during imaging using saline-soaked gauze. The image acquisition time was 2.6 min for both energies. Late imaging time points (20 and 24 h) are not clinically relevant but were used here as comparison data points since the diffusion of contrast agents is presumed to be at diffusion equilibrium at these imaging time points. After microCT imaging, the samples were frozen at −20°C.

2.4 | Digital densitometry

Preceding sample preparation for histological digital densitometry (DD) analysis of the PG content, the contrast agent was washed out from the cartilage tissue by immersing the samples in PBS for a total of 48 h at 7°C, including the change of the PBS bath after 24 h. MicroCT imaging was conducted to confirm that all contrast agent was washed out from the sample. Next, the samples were prepared for DD from twelve locations corresponding with the biomechanical testing locations. Sample blocks, including two biomechanical testing locations, were extracted with matching distances from the edges of the block to ensure correct locations for DD measurements. The extracted samples were fixed in formalin and subsequently decalcified in EDTA to soften them for histological sectioning. Samples were fixed in paraffin and three DD sections with a thickness of 3 μm from each measurement location were prepared using a microtome.[33] The DD sections were stained using safranin-O and measured with a DD measurement system to quantify the depth-wise PG content in cartilage. Safranin-O is a cationic stain that binds specifically and stoichiometrically to the PGs.[34] The DD measurement system was composed of a light microscope (Nikon Microphot-FXA; Nikon Co.) equipped with a monochromatic light source and a 12-bit CCD camera (ORCA-ER; Hamamatsu Photonics K.K.). System calibration was performed using neutral density filters of 0–3.0 optical density. Before determining the optical density of the cartilage at each biomechanical measurement point, the subchondral bone was manually segmented from the images. Then the optical density profiles perpendicular to the articulating surface were determined and the profiles were interpolated to 100 points. The analysis was performed with a custom-made Matlab script (Matlab 2016b; Mathworks, Inc.). A more detailed description of the biomechanical and histological analysis and results can be found in our previous studies.[30,33]

2.5 | Data analysis

MicroCT images were coregistered by first delineating the bone volumes using Stradwin (v. 5.2, Department of Engineering, University of Cambridge) and subsequently matching the orientations of the bone volumes with that of the 0-min, 90 kV baseline image using an open-source software wxRegSurf (v. 16, Department of Engineering, University of Cambridge, UK). After co-registration, the cartilage volumes were traced using ITK-SNAP software (v. 3.8.0, www.itksnap.org) and a custom-made MATLAB script was used to calculate the partitions of iodine and gadolinium in the cartilage based on the equations described below.

The concentrations of two components in a mixture can be solved based on Bragg's additive rule for the mixtures:

$$\alpha_E = \mu_{I,E} C_I + \mu_{Gd,E} C_{Gd}, \quad (1)$$

where α_E is the attenuation coefficient in the medium at an energy E,$\mu_{I,E}$, and $\mu_{Gd,E}$ the mass attenuation coefficients, and C_I and C_{Gd} the concentrations of iodine (I) and gadolinium (Gd) in the mixture. From this equation, iodine and gadolinium concentrations can be solved from the dual-contrast images based on the X-ray attenuation with two tube voltages (here 90 and 50 kV) as follows:

$$C_I = \frac{\alpha_{90}\mu_{Gd,50} - \alpha_{50}\mu_{Gd,90}}{\mu_{I,90}\mu_{Gd,50} - \mu_{I,50}\mu_{Gd,90}} \quad (2)$$

$$C_{Gd} = \frac{\alpha_{50}\mu_{I,90} - \alpha_{90}\mu_{I,50}}{\mu_{I,90}\mu_{Gd,50} - \mu_{I,50}\mu_{Gd,90}}. \quad (3)$$

The attenuation of native cartilage tissue was removed by subtracting the images obtained before the contrast agent immersion from the image obtained at each time point with the same energy. The contrast agent partitions were obtained by dividing the contrast agent concentration inside the cartilage with the concentration in the immersion bath.

In addition, depth-wise contrast agent concentration profiles were calculated from the locations of biomechanical testing to investigate potential differences between the contrast agents' partitioning and DD measurement. To calculate depth-wise contrast agent concentration profiles for iodine and gadolinium, cylindrical regions of interest with 1.416 mm diameter were carefully matched with the histological locations based on microCT measurements having X-ray positive markers on top of the histological location and photographs of the samples.[30] The depth-wise concentration distributions were linearly interpolated into 30 points long depth-wise profiles and afterward used to compare with the depth-wise distribution of PG content. Mean values of contrast-agent concentrations were calculated for full cartilage and superficial cartilage (50% of the total cartilage thickness).

Mann–Whitney U test was used to determine whether statistically significant differences occurred between the contrast agent partitions (CA4+ or gadoteridol) in experimental and control samples. Statistical significance of dependence between DD and CA4+ was calculated using

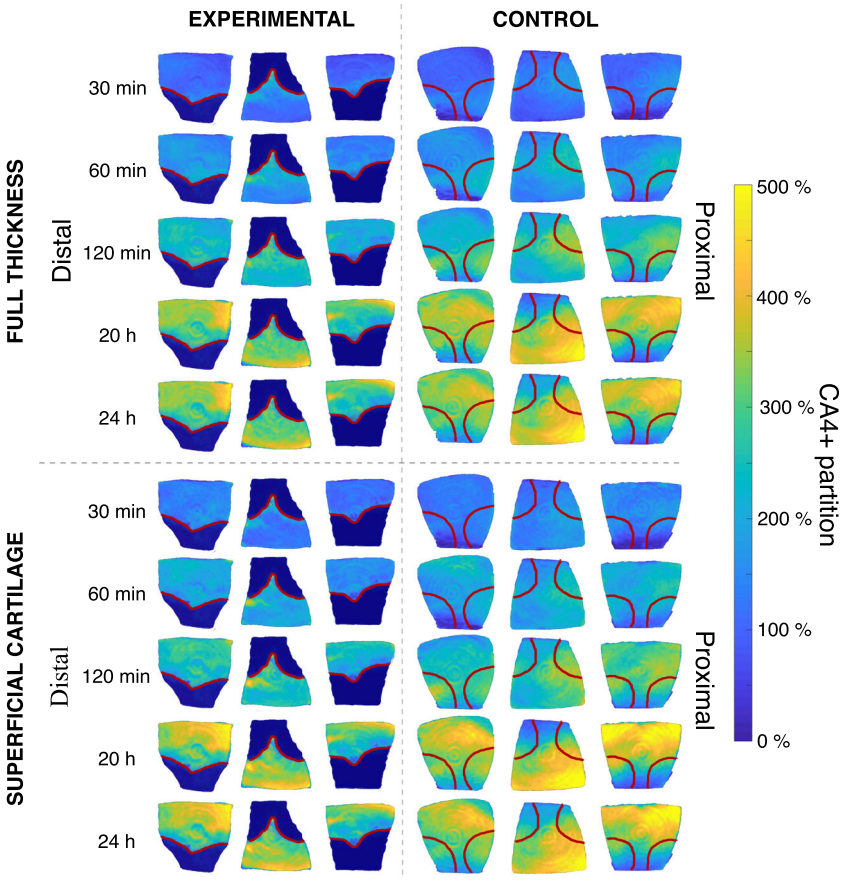

FIGURE 2 Representative partition maps of CA4+ for three experimental and three control samples. The partitions are presented for both full thickness cartilage and for the superficial layer (50% of the total cartilage thickness). Red lines indicate the locations of the lesions in the experimental samples and the corresponding sites in the control samples. Higher partition of CA4+ is seen in the control samples at 20 and 24 h after contrast agent immersion, indicating higher PG content. In experimental samples, the CA4+ partition at 20 and 24 h time points is the lowest near the lesion site and increased when moving further away [Color figure can be viewed at wileyonlinelibrary.com]

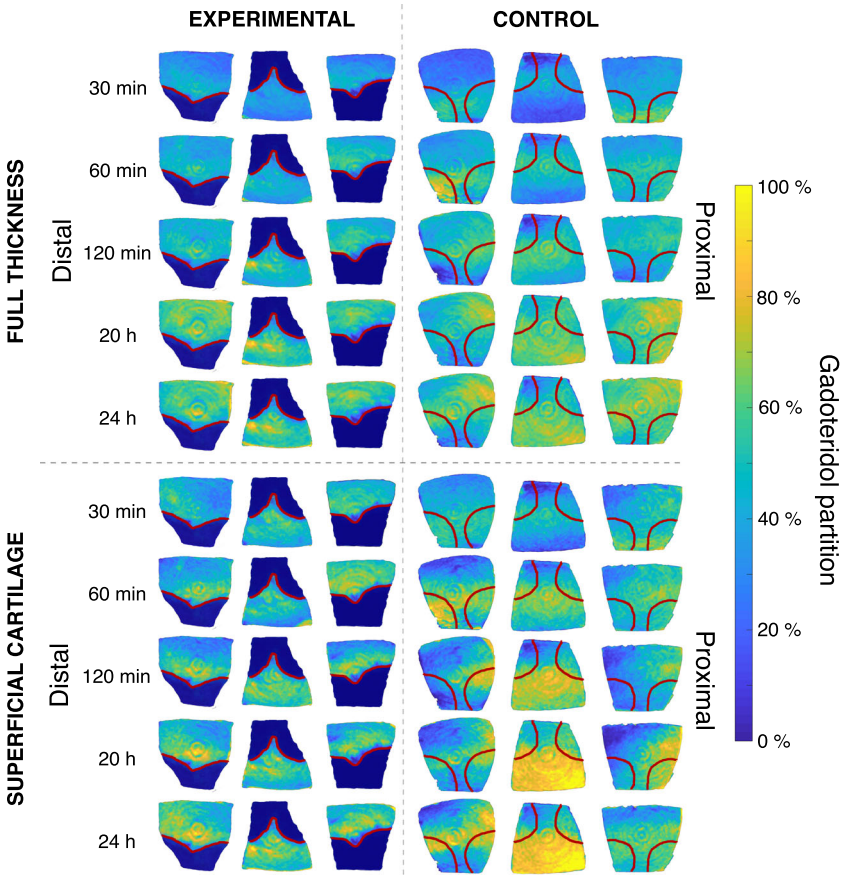

FIGURE 3 Representative partition maps of gadoteridol for three experimental and three control samples. The partitions are presented for both full-thickness cartilage and for the superficial layer (50% of the total cartilage thickness). Red lines indicate the locations of the lesions in the experimental samples and the corresponding sites in the control samples. No distinct differences in gadoteridol partition are seen between the experimental and control samples [Color figure can be viewed at wileyonlinelibrary.com]

Spearman's rank correlation. $p < 0.05$ was considered as the limit for statistical significance. Due to the relatively small sample size and non-normal distribution of the parameters (Shapiro–Wilk test, $p < 0.0001$), nonparametric tests were used. The statistical tests were performed using the SPSS software package (v. 24.0 SPSS Inc., IBM Company).

3 | RESULTS

Mean CA4+ partitions in full thickness cartilage were significantly higher in experimental samples than in control samples at 30 min ($p = 0.004$) and 60 min ($p = 0.028$) after contrast-agent immersion but significantly lower at 20 h ($p < 0.0001$) after immersion. For the superficial cartilage layer, the CA4+ partition was significantly higher at 30 min ($p = 0.001$) and significantly lower at 20 h ($p < 0.0001$) and 24 h ($p < 0.0001$). The partition of gadoteridol in full-thickness cartilage was significantly lower in experimental samples compared with the control samples at 60 min ($p < 0.0001$) and 120 min ($p = 0.002$) after the immersion. In the superficial cartilage layer, gadoteridol partition was lower in experimental samples at 30 min ($p = 0.003$), 60 min ($p < 0.0001$), and 120 min ($p < 0.0001$). No significant differences in gadoteridol partition at 20 or 24 h were found. The partition maps of the full thickness and superficial cartilage layer, respectively, are shown in Figures 2 and 3.

TABLE 1 Spearman's rank correlations of CA4+ partition and reference parameters (optical density, equilibrium, and dynamic moduli)

	Optical density		Equilibrium modulus		Dynamic modulus	
	Full cartilage Thickness	Superficial cartilage	Full cartilage Thickness	Superficial cartilage	Full cartilage Thickness	Superficial cartilage
30 min	−0.148*	−0.304*	−0.137*	−0.289*	−0.078	−0.217*
60 min	−0.177*	−0.325*	−0.150*	−0.341*	−0.102	−0.281*
120 min	0.089	−0.014	0.101	−0.043	0.125	0.015
20 h	0.693*	0.660*	0.635*	0.537*	0.610*	0.537*
24 h	0.627*	0.600*	0.553*	0.482*	0.550*	0.517*

*Indicates that correlation is significant at the level $p < 0.05$.

Twelve biomechanical testing locations were examined from proximal, central, and distal cartilage surrounding the lesions in respect to the anatomical location. Biomechanical testing revealed that in the experimental samples, the equilibrium and dynamic moduli were lower compared with the moduli of the healthy, control samples at all distal locations and most of the central locations ($p < 0.05$). The difference increased toward the distal aspect of the specimens with respect to the joint orientation. The moduli of the control samples decreased toward the medial aspect of the femoral groove. Safranin-O staining revealed a lower overall PG content in the experimental samples compared to the controls. This difference in PG content was greatest near the lesion site and decreased when moving further away in the proximal and distal locations. In contrast, in the central locations, the difference in PG content was greatest farthest away from the lesion site and decreased toward the lesion.

Significant correlations between CA4+ partition and reference parameters (optical density, equilibrium moduli, and dynamic moduli) were obtained at late-diffusion time points of 20 and 24 h (Table 1). Spearman's rank correlations at these time points varied between $\rho = 0.482$ and $\rho = 0.693$. Significant correlations were also obtained at 30 and 60 min time points where the Spearman's rank correlations varied between $\rho = -0.078$ and $\rho = -0.341$.

4 | DISCUSSION

In our previous studies, we showed that QDECT can simultaneously quantify CA4+ and gadoteridol partitions in cartilage, and differentiate healthy from injured cartilage tissue.[23,24,27,27,35] However, the potential of QDECT to detect posttraumatic degeneration in the tissue surrounding a lesion has remained unknown. To investigate this issue, we examined posttraumatic degeneration in equine cartilage surrounding a surgically created and repaired lesion at different imaging time points and evaluated the diagnostic capacity of QDECT in this laboratory study.

CA4+ partition was greater in the experimental samples compared with the control samples at 30 and 60 min after immersion in the contrast agent mixture. In the beginning, the CA4+ diffusion is governed by the lowered steric hindrance but as it reaches equilibrium, the tissue region with the greater PG content dominates the CA4+ partitioning. CA4+ partitions in full-thickness and superficial cartilage layers were significantly higher at the 20 h imaging time point in control samples compared with experimental samples. This result is in line with previous results,[23,24,26,26,27] as the PG content dominates the partition of CA4+ at the late diffusion time points. Unexpectedly, no difference in 24 h time point was found. With the experimental cartilage samples, no apparent difference in either contrast agent partition values between 20 and 24 h existed, indicating that diffusion is at equilibrium or nearly approaching it. In contrast, the contrast agents in control samples did not reach diffusion equilibrium at 20 h as a significant difference was seen between the partition values at 20 and 24 h time points. This incomplete diffusion likely contributes to the observed difference in the partitions between 20 and 24 h in control samples and explains why no statistically significant difference in CA4+ partition could be found between control and experimental samples at the 24 h time point.

Gadoteridol partitions were lower in the experimental than in control samples at the 60 and 120 min time points. Faster diffusion of gadoteridol is consistent with the increases in the water content and permeability of degenerated cartilage. In this context, the lower partition of gadoteridol in the experimental samples at the early diffusion time point is surprising. This result may be explained by the diffusion-related challenges due to possible interactions between gadoteridol and CA4+ molecules. By examining the concentration maps in Figures 2 and 3, the partition of gadoteridol appears to be lower in the areas of high CA4+ partition, suggesting that a repulsive interaction between the two contrast agents may also be occurring. Previous studies have demonstrated that the iodine and gadolinium concentrations can be accurately measured with QDECT,[23,25,27] thus indicating that the technique is functional but may be subject to the above-described challenge in more demanding measurement set-ups. In this study, for example, the size of the samples was bigger, and more tissue is included around the measurement sites whereas the previous studies only included the cartilage with the measured lesions and a small amount of bone underneath.

The present results showed no difference in the partition of the nonionic gadolinium contrast agent between the experimental and control samples at the late-diffusion time points, suggesting that no difference in water content exists. Thus, in the early-diffusion time point, the increased diffusion of the CA4+ with the experimental samples is mostly due to decreased steric hindrance. Alternatively, the differences in water content may be so subtle that these differences are overshadowed by the limitation of conventional microCT, which reduce the sensitivity of QDECT. Conventional microCT systems suffer from beam hardening and other artifacts originating from the polychromatic X-ray beam. The weaknesses of conventional microCT systems can be avoided with synchrotron microCT that implements a narrow energy spectrum, thus minimizing the negative effects of the polychromatic X-ray beam.

A significant positive correlation was seen to exist between the PG content and CA4+ partition at 20 and 24 h time points in both superficial cartilage and full-thickness cartilage. At early diffusion time points (30 and 60 min), the correlations were relatively weak and surprisingly negative. This finding suggests that evaluation of PG content based on CA4+ diffusion in the early diffusion time point in cartilage tissue surrounding the lesion site is unreliable. At 20 and 24 h time points, between equilibrium/dynamic moduli and CA4+ partition, the correlations were positive in both superficial and full cartilage layers. For equilibrium modulus and in the superficial layer for dynamic modulus, weak negative correlations exist in both superficial cartilage and full-thickness at 30 and 60 min time points. The negative correlations are surprising as in previous studies a

positive correlation between CA4+ partition and PG content at early diffusion time points in the lesion sites was reported.[23,26,27] This negative correlation may also arise from the lowered steric hindrance of posttraumatic cartilage, thereby increasing the diffusion of CA4+. Further, reliable quantification of PG and water contents in early-diffusion time points is challenging in species with relatively thick cartilage. In species with thin cartilage (e.g., mice with cartilage thickness of 87 ± 13 μm[36]), mapping of PG and water concentrations is possible after very short diffusion times.

To achieve the most accurate results, data collection with two energies should be performed simultaneously with the shortest possible acquisition time. In this study, the acquisitions at the two energies (90 and 50 keV) were obtained consecutively with the time difference between the acquisition starting points being 4 min 10 s. The acquisition time for one energy was 2.6 min. Immediately after the contrast agent immersion, the diffusion rate of the contrast agent is at its highest, constantly altering the depth-wise partition. Thus, the ongoing diffusion results in an average uptake of the contrast agent over the measurement time rather than an exact uptake value at a certain time point. As the measurement protocols were similar for all samples, the ongoing diffusion has minimal effect on the results or conclusions.

In this study, the samples were images in the air, providing significant contrast, which is unobtainable by imaging joint surfaces ex vivo or in vivo. Loss of contrast at articulating surfaces may lead to incorrect segmentation of cartilage and thus cause misinterpretation of contrast agent partitions. Further, at in vivo imaging, the loss and dilution of contrast agents in the joint capsule occurs rapidly. Thus, the time-dependent contrast agent partitions obtained in this study are greater than can be attained in vivo. The next step forward is to address these limitations in future studies.

In summary, QDECT allows evaluation of cartilage degeneration at diffusion equilibrium and quantification of PG and water contents in the laboratory setting. Additionally, QDECT can differentiate healthy tissue from posttraumatic tissue based on CA4+ partition at 30 and 60 min after contrast agent immersion. However, reliable evaluation of PG content was found challenging at early diffusion imaging time points. The results indicate that evaluation of posttraumatic degeneration in the tissue surrounding the lesions is more complicated than in the lesion site. As indicated above, many challenges still exist and further assessment of QDECT in ex vivo and in vivo models are required to ascertain its limitations and full potential as a diagnostic tool. Given the clinical need for improved diagnostic capabilities for PTOA, the development of QDECT or other such techniques is critical to empower clinicians to choose the optimal treatment modalities for delaying and/or preventing the onset or progression of PTOA.

ACKNOWLEDGMENTS

Amit N. Patwa, PhD is acknowledged for preparing the CA4+. The work was supported by Jorma ja Märtha Sihvola Foundation, Academy of Finland (projects 307932, 285909 and 293970), Doctoral Program in Science, Technology and Computing (SCITECO, University of Eastern Finland), the Jenny and Antti Wihuri Foundation, and the Dutch Arthritis Association (Projects LLP-12 and LLP-22). The funders had no role in study design, data collection and analysis, decision to publish, or preparation of the manuscript.

CONFLICT OF INTERESTS

Dr. Grinstaff reports a patent pending on CA4+ composition. The other authors declare that there are no conflict of interests.

AUTHOR CONTRIBUTIONS

The conception and design of the study was done by Annina EA. Saukko, Irina AD. Mancini, Jetze Visser, Harold Brommer, P Rénévan van Weeren, Jos Malda, Mark W. Grinstaff, Harrie Weinans, and Juha Töyräs. Nikae CR. te Moller, Irina AD. Mancini, Jetze Visser, Harold Brommer, P Rénévan van Weeren, Jos Malda, and Jaakko K. Sarin participated in the sample collection. Biomechanical measurements were performed by Jaakko K. Sarin and Nikae CR. te Moller. Digital densitometry measurements were conducted by Jaakko K. Sarin. Annina EA. Saukko performed microCT measurements. Data analysis was done by Annina EA. Saukko, Olli Nykänen, and Mikko J. Nissi. The data interpretation was done by all the authors. Original draft preparation was done by Annina EA. Saukko and Juha Töyräs. All the authors have critically reviewed and approved the manuscript.

DATA AVAILABILITY STATEMENT

The datasets used and/or analyzed during the current study are available from the corresponding author on reasonable request.

ORCID

Annina E. A. Saukko http://orcid.org/0000-0001-8678-4675
Olli Nykänen http://orcid.org/0000-0001-7329-3463
Jaakko K. Sarin https://orcid.org/0000-0002-6237-9015
Mikko J. Nissi https://orcid.org/0000-0002-5678-0689
Nikae C. R. te Moller http://orcid.org/0000-0001-8675-330X
P. Réné van Weeren https://orcid.org/0000-0002-6654-1817
Mark W. Grinstaff http://orcid.org/0000-0002-5453-3668

REFERENCES

1. Anderson DD, Chubinskaya S, Guilak F, et al. Posttraumatic osteoarthritis: improved understanding and opportunities for early intervention. *J Orthop Res*. 2011;29(6):802-809.
2. Olson SA, Furman BD, Kraus VB, Huebner JL, Guilak F. Therapeutic opportunities to prevent post-traumatic arthritis: lessons from the natural history of arthritis after articular fracture. *J Orthop Res*. 2015;33(9):1266-1277.
3. Li X, Pedoia V, Kumar D, et al. Cartilage T1ρ and T2 relaxation times: longitudinal reproducibility and variations using different coils MR systems and sites. *Osteoarthr Cartil*. 2015;23(12):2214-2223.
4. Link TM, Neumann J, Li X. Prestructural cartilage assessment using MRI. *J Magn Reson Imaging*. 2017;45(4):949-965.
5. Lakin BA, Snyder BD, Grinstaff MW. Assessing cartilage biomechanical properties: techniques for evaluating the functional performance of cartilage in health and disease. *Annu Rev Biomed Eng*. 2017;19(1):27-55.
6. Kokkonen HT, Aula AS, Kröger H, et al. Delayed computed tomography arthrography of human knee cartilage in vivo. *Cartilage*. 2012;3(4):334-341.

7. Myller KA, Turunen MJ, Honkanen JT, et al. In vivo contrast-enhanced cone beam CT provides quantitative information on articular cartilage and subchondral bone. *Ann Biomed Eng*. 2017;45(3):811-818.
8. Yoo HJ, Hong SH, Choi J-Y, et al. Contrast-enhanced CT of articular cartilage: experimental study for quantification of glycosaminoglycan content in articular cartilage. *Radiology*. 2011;261(3):805-812.
9. Stewart RC, Honkanen JTJ, Kokkonen HT, et al. Contrast-enhanced computed tomography enables quantitative evaluation of tissue properties at intrajoint regions in cadaveric knee cartilage. *Cartilage*. 2016;8:391-399.
10. Kokkonen HT, Suomalainen J-S, Joukainen A, et al. In vivo diagnostics of human knee cartilage lesions using delayed CBCT arthrography. *J Orthop Res*. 2014;32(3):403-412.
11. Silvast TS, Kokkonen HT, Jurvelin JS, Quinn TM, Nieminen MT, Töyräs J. Diffusion and near-equilibrium distribution of MRI and CT contrast agents in articular cartilage. *Phys Med Biol*. 2009;54(22):6823-6836.
12. Kallioniemi AS, Jurvelin JS, Nieminen MT, Lammi MJ, Töyräs J. Contrast agent enhanced pQCT of articular cartilage. *Phys Med Biol*. 2007;52(4):1209-1219.
13. Stewart RC, Bansal PN, Entezari V, et al. Contrast-enhanced CT with a high-affinity cationic contrast agent for imaging ex vivo bovine, intact ex vivo rabbit, and in vivo rabbit cartilage. *Radiology*. 2013;266(1):141-150.
14. Joshi NS, Bansal PN, Stewart RC, Snyder BD, Grinstaff MW. Effect of contrast agent charge on visualization of articular cartilage using computed tomography: exploiting electrostatic interactions for improved sensitivity. *J Am Chem Soc*. 2009;131(37):13234-13235.
15. Palmer AW, Guldberg RE, Levenston ME. Analysis of cartilage matrix fixed charge density and three-dimensional morphology via contrast-enhanced microcomputed tomography. *Proc Natl Acad Sci USA*. 2006;103(51):19255-19260.
16. Lusic H, Grinstaff MW. X-ray-computed tomography contrast agents. *Chem Rev*. 2013;113(3):1641-1666.
17. Lin PM, Chen C-TC, Torzilli PA. Increased stromelysin-1 (MMP-3), proteoglycan degradation (3B3- and 7D4) and collagen damage in cyclically load-injured articular cartilage. *Osteoarthr. Cartil*. 2004;12(6):485-496.
18. Buckwalter JA. Mechanical injuries of articular cartilage. *Iowa Orthop J*. 1992;12:50.
19. Silvast TS, Jurvelin JS, Aula AS, Lammi MJ, Töyräs J. Contrast agent-enhanced computed tomography of articular cartilage: association with tissue composition and properties. *Acta Radiol*. 2009;50(1):78-85.
20. Bansal PN, Stewart RC, Entezari V, Snyder BD, Grinstaff MW. Contrast agent electrostatic attraction rather than repulsion to glycosaminoglycans affords a greater contrast uptake ratio and improved quantitative CT imaging in cartilage. *Osteoarthr. Cartil*. 2011;19(8):970-976.
21. Lakin BA, Grasso DJ, Stewart RC, Freedman JD, Snyder BD, Grinstaff MW. Contrast enhanced CT attenuation correlates with the GAG content of bovine meniscus. *J Orthop Res*. 2013;31(11):1765-1771.
22. Lakin BA, Grasso DJ, Shah SS, et al. Cationic agent contrast-enhanced computed tomography imaging of cartilage correlates with the compressive modulus and coefficient of friction. *Osteoarthr. Cartil*. 2013;21(1):60-68.
23. Saukko AEA, Turunen MJ, Honkanen MKM, et al. Simultaneous quantitation of cationic and non-ionic contrast agents in articular cartilage using synchrotron microCT imaging. *Sci Rep*. 2019;9(1):1-9.
24. Honkanen MKM, Matikka H, Honkanen JTJ, et al. Imaging of proteoglycan and water contents in human articular cartilage with full-body CT using dual contrast technique. *J Orthop Res*. 2019;37(5):1059-1070.
25. Bhattarai A, Honkanen JTJ, Myller KAH, et al. Quantitative Dual Contrast CT Technique for Evaluation of Articular Cartilage Properties. *Ann Biomed Eng*. 2018;46(1038):1-9.
26. Honkanen MKM, Saukko AEA, Turunen MJ, et al. Triple contrast CT method enables simultaneous evaluation of articular cartilage composition and segmentation. *Ann Biomed Eng*. 2020;48(2):556-567.
27. Honkanen MKM, Saukko AEA, Turunen MJ, et al. Synchrotron microCT reveals the potential of the dual contrast technique for quantitative assessment of human articular cartilage composition. *J Orthop Res*. 2020;38(3):563-573.
28. Qu C, Hirviniemi M, Tiitu V, Jurvelin JS, Töyräs J, Lammi MJ. Effects of freeze-thaw cycle with and without proteolysis inhibitors and cryopreservant on the biochemical and biomechanical properties of articular. *Cartilage. Cartilage*. 2014;5(2):97-106.
29. Bekkers JE, Tsuchida AI, van Rijen MH, et al. Single-stage cell-based cartilage regeneration using a combination of chondrons and mesenchymal stromal cells. *Am J Sports Med*. 2013;41(9):2158-2166.
30. Sarin JK, Nykänen O, Tiitu V, et al. Arthroscopic determination of cartilage proteoglycan content and collagen network structure with near-infrared spectroscopy. *Ann Biomed Eng*. 2019;47(8):1815-1826.
31. Hayes WC, Keer LM, Herrmann G, Mockros LF. A mathematical analysis for indentation tests of articular cartilage. *J Biomech*. 1972;5(5):541-551.
32. Danso EK, Mäkelä JT, Tanska P, et al. Characterization of site-specific biomechanical properties of human meniscus—importance of collagen and fluid on mechanical nonlinearities. *J Biomech*. 2015;48(8):1499-1507.
33. Nykänen O, Sarin JK, Ketola JH, et al. T2* and quantitative susceptibility mapping in an equine model of post-traumatic osteoarthritis: assessment of mechanical and structural properties of articular cartilage. *Osteoarthr. Cartil*. 2019;27(10):1481-1490.
34. Kiviranta I, Jurvelin J, Säämänen A-M, Helminen HJ. Microspectrophotometric quantitation of glycosaminoglycans in articular cartilage sections stained with Safranin O. *Histochemistry*. 1985;82(3):249-255.
35. Bhattarai A, Honkanen JTJ, Myller KAH, et al. Quantitative dual contrast CT technique for evaluation of articular cartilage properties. *Ann Biomed Eng*. 2018;46(7):1038-1046.
36. Malda J, de Grauw JC, Benders KEM, et al. Of mice, men and elephants: the relation between articular artilage thickness and body mass. *PLOS One*. 2013;8(2):e57683.

How to cite this article: Saukko AEA, Nykänen O, Sarin JK, et al. Dual-contrast computed tomography enables detection of equine posttraumatic osteoarthritis in vitro. *J Orthop Res*. 2022;40:703-711. https://doi.org/10.1002/jor.25066